#### Viacheslav Loveikin

Professor

National University of Life and Environmental Sciences of Ukraine Department of Machines and Equipment Design Ukraine

# Yuriy Romasevych

Professor National University of Life and Environmental Sciences of Ukraine Department of Machines and Equipment Design Ukraine

#### **Borys Bakay**

Associate Professor Ukrainian National Forestry University Department of Forest Engineering Ukraine

#### Ihor Rudko

Associate Professor Ukrainian National Forestry University Department of Forest Engineering Ukraine

#### Ivan Radiak

PhD student Ukrainian National Forestry University Department of Forest Engineering Ukraine

# Modelling and Dynamic Analysis of an Integrated Hydraulic Forest Crane-Winch System for Timber Extraction

This paper details the dynamic modelling and analysis of an integrated hydraulic forest crane-winch system used for timber extraction, concentrating on transient behaviour during winch activation from rest. A comprehensive mathematical model was developed to capture the coupled dynamics of the winch drum rotation, the crane boom, and the suspended timber log, using the Lagrangian formulation. The resulting system of coupled, nonlinear second-order ordinary differential equations was solved numerically using custom algorithms. Dynamic analysis revealed transient overloading: peak drive torque, rope tension, and boom elastic force exceeded steady-state values by factors of 4.47, 2.44, and 2.91, respectively. High-frequency damped oscillations superimposed on lowfrequency payload sway were identified, attributed to the abrupt drive torque application. This research highlights the necessity of dynamic analysis for predicting significant stress amplification in such systems and provides a framework for characterising transient loads, indicating smoother start-up strategies are essential for improving system reliability and efficiency.

**Keywords:** modelling, hydraulic forest crane, winch, timber extraction, dynamic lads, transient analysis.

#### 1. INTRODUCTION

The sustainable and efficient management of forest resources is a cornerstone of modern forestry engineering, demanding robust and effective engineering solutions for timber harvesting and transportation [1,2]. Central in timber harvesting production processes is the handling of timber logs, which often involves manipulating substantial masses across challenging and unstructured terrains [3,4].

The mechanised timber extraction process is funda mental to modern timber harvesting [5], relying heavily on specialised machinery to handle substantial log masses within often challenging operational environments [6]. Hydraulic forest cranes, typically mounted on carriers such as forwarders, skidders or trailers, are pivotal in these operations, executing loading, sorting, and short-range transport cycles [7]. To enhance operational scope, particularly for retrieving timber from areas inaccessible to the primary machine or across significant distances, winch systems are frequ-ently integrated with the formation of complex multi-functional equipment (Figure 1). These winch-assist or tethering functionalities, often based on the crane's chassis, allow for initial log gathering or machine stabilisation on steep slopes [8, 9]. While offering increased versatility, the consolidation of a hydraulic manipulator and a rope winch system onto a single platform introduces

Received: May 2025, Accepted: September 2025 Correspondence to: Ivan Radiak, Department of Forest Engineering, Ukrainian National Forestry University, General Chuprynka St 103, Lviv, 79057, Ukraine E-mail: ivan.radiak@nltu.edu.ua

doi: 10.5937/fme2504625L

significant mechanical engineering complexities, particularly concerning the system's dynamic response under load

The dynamic behaviour of a hydraulic forest crane during timber extraction is inherently complex [7], involving the controlled motion of multiple articulated links under the influence of substantial, time-varying payload forces [10.11]. When a winch system is integrated and operated concurrently or sequentially, the dynamic interactions intensify. Significant rope tensile forces are generated during winch operation (hauling, braking), imposing reaction loads onto the crane's structure, which serves effectively as the anchor machine [1,6]. Operational tasks, such as crane slewing or luffing while winching, or the negotiation of obstacles during tethered movement of logs, can induce pronounced peak tensile force events [1]. The inherent dynamic nature of forest machines interacting with the terrain and payload [12,13] means that transient loads, arising from log pick-up, impacts, or sudden changes in rope tension (e.g., due to dynamic braking mechanisms or threshold settings in the winch control [14]), are commonplace. Furthermore, the forest crane itself acts as a pendulum, contributing further dynamic forces to the boom structure [15].

These dynamic loads and the resultant vibrations have profound implications for the mechanical design and the robust performance of the equipment. Fluctuating stresses within the boom sections [11], slewing mechanism, joints [16], and winch components [17] directly affect fatigue life and the risk of structural failure. The inherent flexibility of the crane's long boom structure [18], combined with the elasticity of the winch wire rope [6], provides pathways for vibration, which

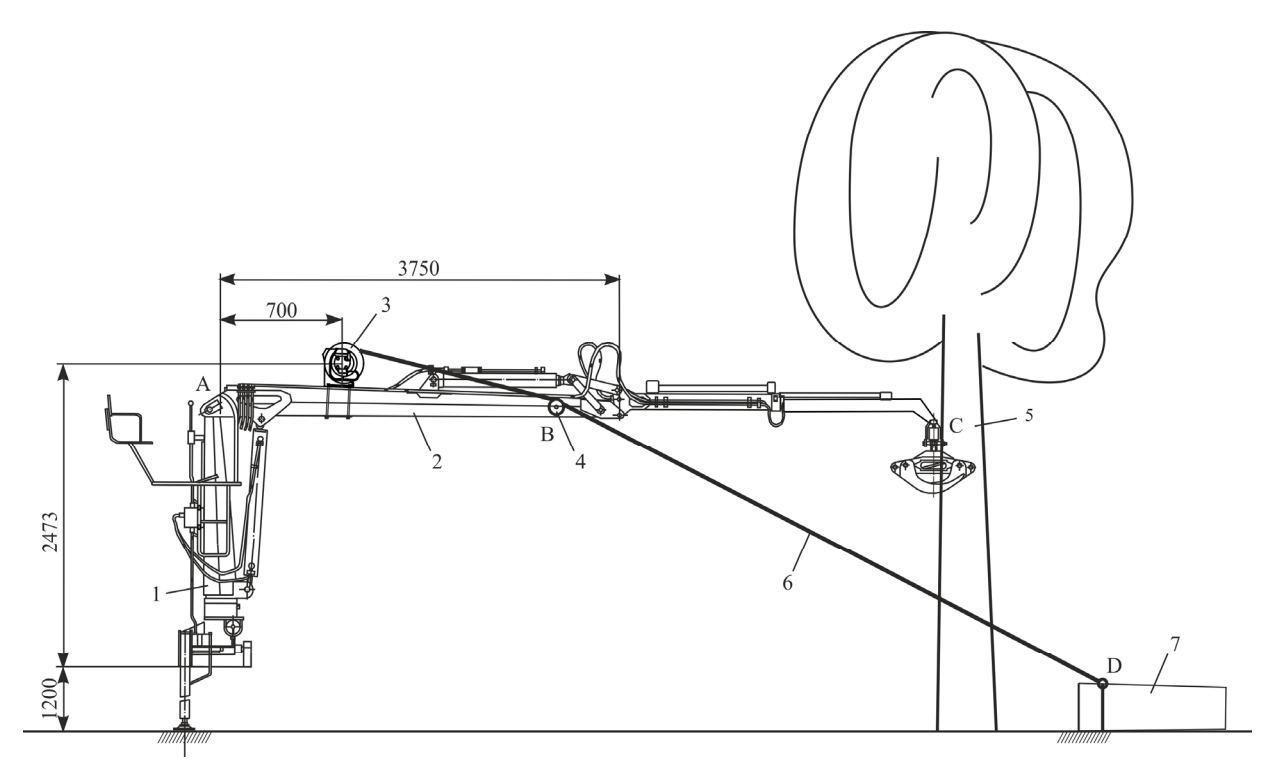


Figure 1. Schematic representation of the forest crane used for timber extraction

can be excited by actuator inputs, payload motion, or interaction with the terrain and potential obstacles. Such vibrations not only degrade the precision required for efficient log handling but can also affect operator comfort and potentially compromise the machine's overall stability, especially when operating near capacity limits or on uneven ground. Exceeding safety limits, such as the Safe Working Load of the winch rope [19], is a critical safety concern. Therefore, a detailed dynamic analysis, accounting for the coupled behaviour of the forest crane and integrated winch during representative harvesting operations, is indispensable. Accurate modelling allows for the prediction of system response, the quantification of internal loads and stresses, the characterisation of vibrational behaviour, and the assessment of stability. This forms the essential basis for structural optimisation, rational component selec-tion, and the development of advanced control systems aimed at enhancing both productivity and safety in mechanised timber extraction. Consequently, the focus of this research is the development of a representative model for such an integrated hydraulic forest crane-winch system and its dynamic analysis, particularly examining the coupled dynamics and the influence of operational parameters.

Specifically, during the transient phase associated with the initiation of the log hauling cycle (start-up), oscillatory processes arise within the components of the timber extraction system, leading to a considerable amplification of dynamic loads. These effects can compromise operational reliability and elevate energy expenditure. Therefore, the accurate determination of these actual dynamic loads and the thorough investigation of the associated vibrational phenomena within the structural elements during the log hauling operation constitute a significant and relevant engineering task.

#### 2. LITERATURE REVIEW

The development of equipment for timber extraction [20] has gained significant attention in forestry engineering, driven by the need to improve operational efficiency while minimising environmental impact [5]. Traditional ground-based extraction systems, though widespread, often result in soil compaction and ecosystem disruption, particularly in sensitive terrains [4, 8]. Cable-based extraction systems, such as those employing winches [21] or forest cranes [22], provide a viable alternative by minimising soil disturbance [4,23]. Recent studies underscore the economic and ecological benefits of cable-yard systems, particularly in flat or soil-sensitive regions, where productivity and costefficiency can be comparable to ground-based methods [2,5]. However, challenges persist in optimising dyna mic stability and energy consumption during transient operations, necessitating advancements in system design and control methodologies [6,7,10,11,15,16,18].

The evolution of forestry equipment has emphasised the integration of hydraulic drives [11,16] due to their high torque capabilities and adaptability to rugged environments. Hydraulic winches, for instance, are widely employed in timber extraction [21], offering robust performance in steep terrains [6,9]. Despite their advantages, hydraulic systems are often associated with energy inefficiencies and dynamic load fluctuations during start-up and braking phases [17,24]. Recent innovations, such as electro-hydraulic hybrid drives, aim to mitigate these issues by combining hydraulic power with electric precision [25]. The proposed extraction system, which integrates a hydraulic winch mounted on a forest crane, aligns with this trend, leveraging hydraulic robustness while addressing dynamic challenges through advanced modelling.

Several established methodologies exist for the dynamic modelling of complex mechanical systems, including those with significant structural flexibility, which are broadly applicable to the timber extraction system under consideration. Techniques commonly employed in the analysis of hydraulic manipulators, which share characteristics with forest cranes, include the assumed modes method (AMM), the finite element method (FEM), the lumped parameter method (LPM), and the transfer matrix method (TMM) [26,27]. AMM represents flexibility using a truncated series of mode shapes, often leading to lower-order models suitable for control design, but requires careful selection of appropriate modes and boundary conditions. FEM offers versatility in handling complex geometries and nonuniform properties, providing detailed stress and strain information, but typically results in high-order models that can be computationally intensive for dynamic simulation or real-time control [26]. LPM provides an intuitive approach by discretising the system into interconnected masses, springs, and dampers, but may struggle to accurately represent distributed flexibility and requires careful parameter identification [26]. The choice of method often involves a trade-off between model fidelity and computational feasibility, depending on the specific analysis objectives.

A critical component requiring careful modelling is the hydraulic crane's boom structure. While simpler analyses might treat the boom sections as rigid bodies. the significant length and reach required for forestry operations mean that structural flexibility cannot always be neglected, particularly for lightweight designs or during high-speed manoeuvres [28]. Techniques developed for flexible-link manipulators are directly relevant here, often employing beam theories such as Euler-Bernoulli (for slender sections where shear deformation is minimal) or Timoshenko (which accounts for shear deformation and rotary inertia, more suitable for thicker sections or higher-frequency dynamics) in conjunction with AMM or FEM [27]. Incorporating boom flexibility introduces vibration modes that can interact with payload oscillations and hydraulic system dynamics, complicating control and potentially impacting structural fatigue life. Furthermore, factors such as varying log payloads, the dynamic characteristics of the hydraulic actuation system, joint clearances, and friction significantly influence the overall system response and must be appropriately accounted for within the dynamic model to achieve accurate predictions of real-world behaviour. The investigation of these coupled dynamic phenomena, particularly during demanding operational phases like log hauling start-up, remains an important area for enhancing the design and operational efficiency of timber extraction systems based on hydraulic cranes.

A crucial aspect of forest crane modelling involves accurately representing structural flexibility [29]. The forest crane's boom, modelled as an elastic beam with lumped mass, reflects a common approach in dynamic analyses [30]. Several studies [31-34] demonstrate that discretising continuous structures into equivalent mass-spring-damper systems reduces computational complexity while maintaining dynamic accuracy. For instance, the study in [32] modelled multi-section telescopic

crane booms using Rayleigh's method to analyse their vibrational characteristics. The method shows reliable results with minimal error of 4.6% compared to finite element analysis, confirming its efficiency for structural assessment. Similarly, study [34] develops and validates a comprehensive mathematical model for analysing the dynamics of boom cranes, incorporating key factors such as load, drive flexibility, and crane link properties. Utilising advanced formalism and computational tools, the model provides insights into the dynamic behaviour of the crane, assessed through a formalism of joint coordinates and Lagrange equations of the second kind. The findings contribute to a deeper understanding of the influence of structural and operational parameters in crane dynamics.

Lagrangian dynamics remain a cornerstone for modelling multi-body systems with interconnected rigid and elastic components. The existing modelling methodology involves a system of nonlinear differential equations to describe the coupled motion of the crane boom, hydraulic system and log [35]. The Lagrange method removes the interaction forces between neighbouring links and offers an organised approach to derive the motion equations for the entire system [26]. Researchers [16,29,31] have validated the efficacy of Lagrange's equations in describing forestry manipulators, particularly when integrating hydraulic actuation and elastic linkages.

Conducted comparative analyses of dynamic loads in winch systems reveal consistent patterns of high-frequency oscillations in drive mechanisms, and low-frequency sway in wire ropes and loads [3,11,24]. Peak tensile forces in the winch wire ropes were during timber extraction and movement tethered harvesting machine [1,17], which correlates with abrupt torque changes in hydraulic motors [24]. These findings parallel the study's results, where start-up phases induced transient overloads significantly exceeded of steady-state values in the winch drive [1,36]. Furthermore, the damping of high-frequency vibrations in the forest cranes' elastic elements underscores the importance of dissipative components in stabilising system behaviour [22,33].

The integration of numerical methods, such as finite difference [37] and Runge-Kutta algorithms [33], has proven indispensable for simulating nonlinear dynamics [26,38]. Research results have demonstrated the utility of numerical solvers in system design for forestry cranes [7,33], and numerous examples employing programe mathematics toolbox to validate offshore crane models are also known [39-41]. In those studies, numerical solutions of the derived equations facilitated the identification of critical transient phenomena, such as the rapid attenuation of boom oscillations within four seconds and prolonged load sway persisting beyond twelve seconds. Also, these results are consistent with the findings of [11, 15], who realised optimised start-up protocols for the loading equipment to reduce energy consumption and mechanical stress.

In conclusion, the literature survey underscores the viability of hydraulic-driven technical systems for timber extraction, provided dynamic challenges are addressed through rigorous modelling. The present

study advances this domain by integrating Lagrangian mechanics, lumped-parameter approximations, and numerical analysis to optimise the design and operation of a forest crane-based integrated hydraulic system, providing a framework for improving reliability and efficiency in forest harvesting.

#### 3. METHODOLOGY

The methodology employed in this study addresses the research objectives through a structured approach encompassing dynamic modelling, mathematical derivation, and numerical analysis. To achieve this objective, the following research tasks were formulated: 1) to establish a dynamic model (analytical representation) that accounting for the coupled motion of the principal elements within the integrated hydraulic forest cranewinch system used for timber extraction; 2) to derive the mathematical model describing the system's coupled motion based on the established dynamic model, employing Lagrange's equations of the second kind (the Lagrangian formulation); 3) to conduct a dynamic analysis, utilising the derived mathematical model, to investigate the simultaneous (coupled) dynamic behaviour of the integrated system elements during operational scenarios.

The formulated tasks are driven by the need to accurately understand, predict, and ultimately mitigate the complex dynamic loads and vibrational phenomena inherent in such coupled systems, particularly during demanding operational phases identified as critical in the literature and preliminary analysis. The findings are expected to contribute to the refinement of modelling approaches for forestry machinery, facilitate the development of advanced control strategies, and enhance the reliability and efficiency of timber extraction processes.

## 3.1 Dynamic Model Development

The initial step involved constructing a dynamic model (analytical representation) of the timber extraction system designed for log hauling. This model conceptualises the system as an interconnected multi-body dynamic entity, explicitly accounting for the coupled motion of its principal elements: the hydraulic winch drum, the forest crane boom structure, the moving timber log, and the winch rope connecting the log to the drum. Consistent with established approaches for analysing the dynamics of manipulators and forest crane structures, particularly where transient behaviour and flexibility occur [3,28], key simplifications were adopted to render the model tractable yet representative.

Specifically, the crane boom's structural flexibility, primarily in bending, was incorporated using a lumped parameter approach. An equivalent single-degree-of-freedom model, derived using Rayleigh's energy equivalence principle [27], was employed to capture the dominant fundamental mode of vibration expected during dynamic loading events like winch start-up. This approach allows for the representation of the boom's distributed mass and stiffness properties through an equivalent lumped mass and spring constant at a representative point (e.g., the sheave location), facili-

tating the analysis of high-frequency oscillations [11, 15]. The timber (logs) was modelled as a physical load, connected to the pulley via the winch rope. For this stage of analysis, the winch rope was treated as extensible and of variable length, focusing the investigation on the primary payload swing dynamics and structural interactions. The winch drum was modelled as a rotating inertia driven by the hydraulic motor torque. Appropriate coordinate systems were established to define the system's configuration, resulting in a model characterised by three key generalised coordinates.

#### 3.2 Mathematical Model Formulation

Based on the established dynamic model, the mathematical model describing the system's coupled motion was derived systematically using Lagrange's equations of the second kind. This Lagrangian formulation was chosen due to its effectiveness in handling multi-body systems with both rigid and elastic components, as frequently employed in manipulator dynamics [11,26,27]. The derivation involved formulating the system's total kinetic energy (incorporating translational and rotational kinetic energies of the drum, equivalent boom mass, and log) and total potential energy (including gravitational potential energy of the log and boom mass, and the strain energy stored in the equivalent boom spring).

Generalised forces corresponding to each generalised coordinate were identified. These included the driving torque applied to the winch drum by the hydraulic system, gravitational forces acting on the components, and dissipative forces representing potential damping sources (e.g., structural damping within the boom, viscous friction in the winch mechanism, resistance to log movement). Applying the standard Lagrangian procedure resulted in a set of three coupled, second-order, nonlinear ordinary differential equations (ODEs) governing the time evolution of the generalised coordinates. These equations intrinsically capture the dynamic coupling between the winch rotation, boom vibration, and payload swing.

# 3.3 Dynamic Analysis

The dynamic analysis was conducted by numerically solving the derived system of nonlinear ODEs. This computational approach is necessary due to the complexity and nonlinearity of the mathematical model, precluding straightforward analytical solutions, particularly for transient behaviour. Simulations were performed using custom algorithms developed within the Wolfram Mathematica environment, employing robust numerical integration schemes a variable-step Runge-Kutta solver suitable for potentially stiff systems encountered in mechanical dynamics [7,11,16].

The primary focus of the dynamic analysis was the investigation of the system's transient response during the critical log hauling cycle start-up phase. This phase was selected based on both practical relevance and indications from literature suggesting significant dynamic load amplification during such initiation periods [6, 15]. Simulations were configured to model the application of drive torque to the winch drum from rest,

considering representative parameters for the crane geometry, log mass, winch characteristics, and initial conditions. Key output variables were monitored and analysed, including: winch drum angular velocity and acceleration, driving torque profile, boom deflection and velocity, log swing angle and angular velocity, and, crucially, the calculated tensile force within the winch rope. The results of these simulations were used to characterise the oscillatory processes, quantify the peak dynamic loads experienced by system components relative to steady-state values, assess the time scales of vibration damping, and evaluate the influence of system parameters on the overall dynamic behaviour.

#### 4. FORMULATION OF MODEL

This study presents the results of a modelling-based investigation of a timber extraction system comprising a hydraulic forest crane and a winch. To assess its design, operational modes, and potential for performance enhancement, a mathematical model of the system was developed and subjected to dynamic analysis.

Specialised technical equipment for timber extraction has been developed, comprising a hydraulic forest crane configured for pulling logs (see Figure 1). The proposed technical equipment assumes that the boom 2 of the forest crane rests against a tree trunk 5, forming a rigid system together with the tree. A winch 3 is rigidly mounted on the boom 2, closer to the crane's slewing column 1, with its traction rope 6 routed through a guide pulley 4 and connected to the payload 7. The extracted payload 7 consists of one or more round timber materials. When the winch 3 is activated, the rope 6 is wound onto the drum, pulling the logs towards the forest crane.

In Figure 2, the kinematic diagram of the proposed technical equipment for timber extraction is presented. In this schematic, the boom of the forest crane is represented as beam 2, supported at two points: one by the forest crane column 1 and the other by the trunk of a standing tree 5, against which the boom is braced. At a distance  $b_1$  from support A, a traction winch 3 is mounted on the boom, with its wire rope 6 routed through a guide pulley 4 and connected to the log 7 at point D. When the winch is activated, the log is pulled towards the loader. The guide pulley 4 is positioned on the boom at a distance a from support A.

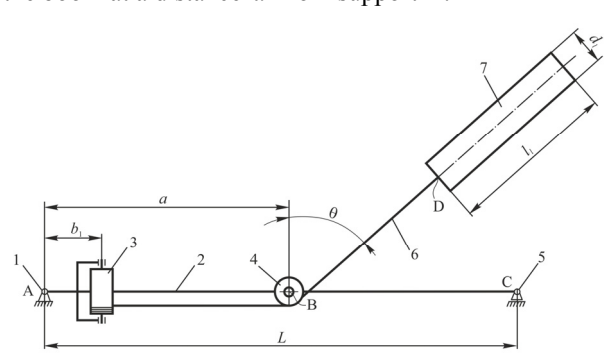


Figure 2. Kinematic diagram of the integrated hydraulic forest crane-winch system used for timber extraction

To confirm the operational feasibility of the proposed integrated hydraulic forest crane-winch system used

for logs extraction, a dynamic analysis will be conducted during its operation. In this analysis, the boom 2 and the wire rope 6 are assumed to possess elastic-dissipative properties, while the components of the winch 3, the guide pulley 4, and the log 7 are considered as absolutely rigid bodies. The elastic-dissipative and inertial properties of the forest crane boom will be represented by an equivalent lumped-parameter model consisting of a discrete mass with associated elastic and dissipative elements.

Assuming that the mass and stiffness of the boom are uniformly distributed along its length, the mass function can be expressed as m(x) = const and the bending stiffness as EI(x) = const. Here,  $E = 2.1 \times$ 10<sup>5</sup> MPa represents the modulus of elasticity of the steel used for the boom, while I(x) denotes the area moment of inertia of the boom's cross-section relative to the bending axis. The forest crane boom possesses an infinite number of degrees of freedom and, correspondingly, an infinite number of natural vibration modes. The Rayleigh method is employed to approximate the boom as a beam with a single equivalent discrete mass  $m_n$  and a single generalised coordinate z(x), with an associated generalised stiffness  $c_n$ . Under these assumptions, the deflection of the boom at any given point along its length is determined by the following expression

$$u(t) = \psi(x)z(t) \tag{1}$$

where  $\psi(x)$  is the mode shape, representing the ratio of the displacement of any point on the beam to the generalised coordinate z(t). In this formulation, the mode shape of the beam remains unchanged over time, while only the amplitude of its vibrations varies. The mode shape corresponding to the fundamental frequency is chosen and represented as a half-wave sine function

$$\psi(x) = \sin\left(\frac{\pi x}{L}\right) \tag{2}$$

It satisfies the condition of zero deflection at the supports and represents the exact solution for the actual vibration mode of a simply supported beam.

Under these conditions, the generalised mass of the boom located in its middle. To achieve this, the following integral is used

$$m^* = \int_0^L m(x) [\psi(x)]^2 dx = \frac{m_c}{L} \int_0^L \left[ \sin\left(\frac{\pi x}{L}\right) \right]^2 dx$$
 (3)

In the resulting integral, we make the substitution  $\left[\sin\left(\frac{\pi x}{L}\right)\right]^2 = \frac{1}{2}\left[1-\cos\left(\frac{2\pi x}{L}\right)\right]$  as a result we will have

$$m^* = \frac{m_c}{2L} \int_0^L \left[ 1 - \cos\left(\frac{2\pi x}{L}\right) \right] dx = \frac{m_c}{2}$$
 (4)

Now, let us determine the generalised stiffness of the boom

$$c^* = \int_0^L EI(x) [\psi^{II}(x)]^2 dx$$
 (5)

**FME Transactions** 

The second derivative of the mode shape function with respect to the coordinate is found as

$$\psi^{I}(x) = \frac{\pi}{L}\cos\left(\frac{\pi x}{L}\right); \ \psi^{II}(x) = -\left(\frac{\pi}{L}\right)^{2}\sin\left(\frac{\pi x}{L}\right)$$
 (6)

Substituting this into integral (5), we obtain

$$c^* = \left(\frac{\pi}{L}\right)^4 EI \int_0^L \left[\sin\left(\frac{\pi x}{L}\right)\right]^2 dx =$$

$$= \frac{1}{2} \left(\frac{\pi}{L}\right)^4 EI \int_0^L \left[1 - \cos\left(\frac{2\pi x}{L}\right)\right] dx = \frac{\pi^4}{2I^3} EI$$
(7)

Thus, a forest crane boom resting on a tree is represented by a dynamic model in the form of a unit concentrated mass  $m^*$ , which is connected to a fixed support in the middle of the boom by an elastic element with a stiffness coefficient  $c^*$ . Since the force causing the deflection of the boom is not applied at its midpoint but rather at the point where the rope passes through the guiding pulley, it is necessary to determine the equivalent mass and stiffness of the forest crane boom at this specific location. The equivalent mass of the boom at the attachment point of the pulley is determined based on the condition of kinetic energy equivalence between the reduced masses at the pulley attachment point and at the midpoint of the boom

$$\frac{1}{2}m^*\dot{z}^2(t)\left[\sin\left(\frac{\pi L}{2L}\right)\right] = \\
= \frac{1}{2}m_z\dot{z}^2(t)\left[\sin\left(\frac{\pi\alpha}{L}\right)\right]^2$$
(8)

From Eq. (8), the equivalent mass of the boom, reduced to the axis of the guiding pulley attachment, is determined as follows:

$$m_n = m^* \frac{\left[\sin\left(\frac{\pi}{2}\right)\right]^2}{\left[\sin\left(\frac{\pi\alpha}{L}\right)\right]^2} = \frac{m_c}{2\left[\sin\left(\frac{\pi\alpha}{2L}\right)\right]^2}$$
(9)

The equivalent stiffness of the boom at the attachment point of the guiding pulley is determined based on the condition of potential energy equivalence between the reduced masses at the pulley attachment point and at the midpoint of the boom.

$$\frac{1}{2}c^*z^2(t)\left(\frac{\pi}{L}\right)^4 \left[\sin\left(\frac{\pi L}{2L}\right)\right]^2 = \\
= \frac{1}{2}c_nz^2(t)\left(\frac{\pi}{L}\right)^4 \left[\sin\left(\frac{\pi\alpha}{L}\right)\right]^2$$
(10)

From Eq. (10), the stiffness of the boom, reduced to the attachment point of the guiding pulley, is determined

$$c_n = c^* \frac{\left[\sin\left(\frac{\pi}{2}\right)\right]^2}{\left[\sin\left(\frac{\pi\alpha}{L}\right)\right]^2} = \frac{\pi^4}{2L^2} EI \frac{1}{\left[\sin\left(\frac{\pi\alpha}{L}\right)\right]^2}$$
(11)

The traction rope exhibits elastic-dissipative properties; hence, it is modelled as a flexible thread with elastic and dissipative elements. Based on this, the timber extraction system for pulling logs 7, accounting for the winch 3 mounted on the boom 2 of the forest crane, is represented as a discrete dynamic model, as illustrated in Figure 3.

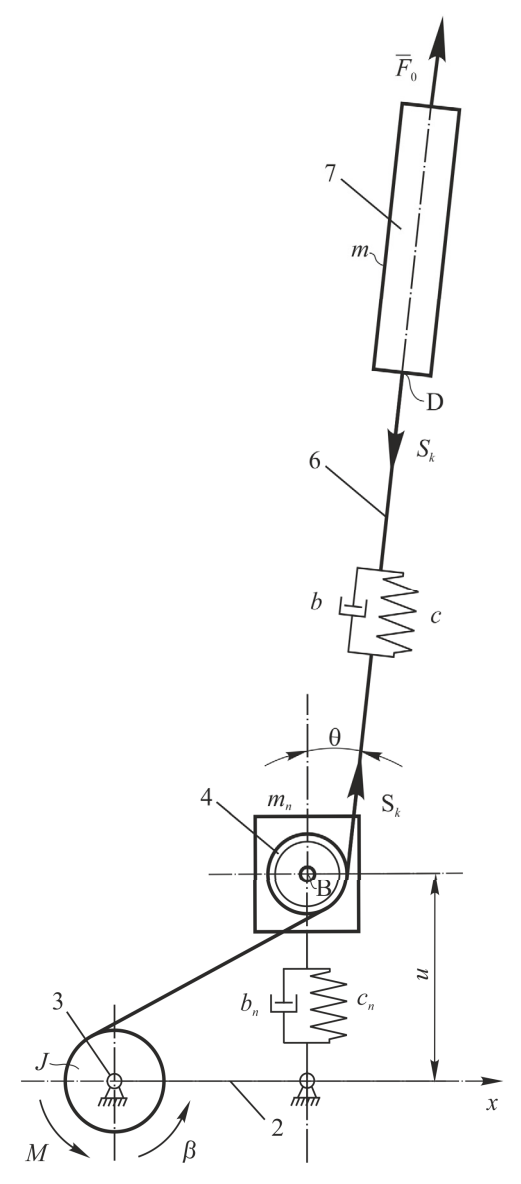


Figure 3. The dynamic model of the integrated hydraulic forest crane-winch system for timber extraction

In Figure 3, the following notations are adopted: M is the driving torque of the winch 3 drive, reduced to the axis of the drive drum; J is the moment of inertia of the winch 3 drive, reduced to the axis of the drive drum;  $m_n$ ,  $c_n$ ,  $b_n$  is the mass of the boom 2, its stiffness coefficient, and damping coefficient, all reduced to the axis of the deflecting pulley 4; c, b is the stiffness and damping coefficients of the rope 6;  $S_k$  is the tension force in the rope 6;  $S_k$  is the tension force of resistance to log 7 movement. In this case, the stiffness coefficient of the rope 6 is determined by the following relationship

$$c = \frac{E_k S_r}{L_k} = \frac{E\pi d^2}{4L_k} \tag{12}$$

where  $E_k = (1.25-1.30) \times 10^5$  MPa is the modulus of elasticity of the rope in tension; d is the diameter of the rope;  $L_k$  is the length of the rope, which varies during the work of the log. However, since only a small displacement of the log is considered during the start-up phase, we approximately assume  $L_k = \text{const}$ ;  $S_r$  is the cross-sectional area of the rope.

The forces acting on the log are shown in Figure 4.

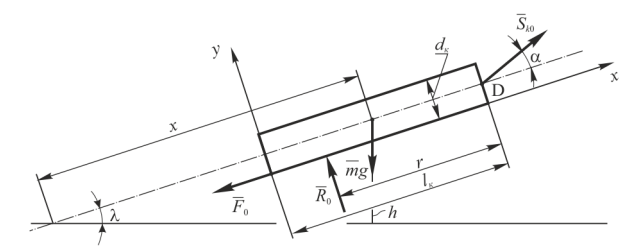


Figure 4. Diagram of the forces acting on the log

The force of resistance to the movement of the log is determined from the conditions of its static equilibrium (Figure 4) and is expressed by the following relation

$$F_0 = f_0 \cdot mg \left( \cos \lambda - \frac{f_0 \cdot \cos \lambda + \sin \lambda}{f_0 \cdot \sin \lambda + \cos \lambda} \sin \alpha \right)$$
 (13)

where  $f_0$  is the coefficient of resistance to the log movement; m is the mass of the log; g is the acceleration due to gravity;  $\lambda$  is the inclination angle of the surface relative to the horizontal along which the log is being pulled; and  $\alpha$  is the angle of the rope inclination relative to the direction of log movement.

Since the actual mechanical characteristic of the hydraulic motor is described by a dependence close to a second-order curve, the driving torque of the winch drive is modelled as a second-order function of the angular velocity of the hydraulic motor shaft and its nominal parameters. As a result, the following expression for the driving torque of the drive, reduced to the axis of rotation of the drive drum, is used [1]:

$$M = \left[ M_p + \left( K \omega_0 - \frac{M_p}{\omega_0} \right) i_w \dot{\beta} - K (i_w \dot{\beta})^2 \right] i_w \eta \qquad (14)$$

$$K = \frac{M_n - M_p \left( 1 - \frac{\omega_n}{\omega_0} \right)}{\omega_0 (\omega_0 - \omega_0)} \qquad (15)$$

Where  $M_p$  and  $M_n$  are the starting and nominal torques of the hydraulic motor, respectively;  $\omega_n$  and  $\omega_0$  are the nominal and synchronous angular velocities of the hydraulic motor shaft;  $i_w$  is the transmission ratio of the winch drive;  $\eta$  is the efficiency of the winch drive.

The dynamic model of the integrated hydraulic forest crane-winch system used for timber extraction, presented in Figures 3 and 4, accounts for the primary rotational motion of the winch drive mechanism, as well as the deformations of the wire rope and the elastic element of the equivalent boom mass. Consequently, the proposed dynamic model has three degrees of freedom. The generalised coordinates used in the dynamic model of the integrated hydraulic forest crane-winch system used for timber extraction are as follows:  $\beta$  is angular

coordinate of the drive drum rotation; u is linear coordinate of the boom deformation at the attachment point of the guiding pulley axis; x linear coordinate of the log displacement.

Based on the developed dynamic model of the integrated hydraulic forest crane-winch system used for timber extraction, a mathematical model has been constructed. To achieve this, the Lagrange equations of the second kind are employed:

$$\frac{d}{dt}\frac{\partial T}{\partial \dot{\beta}} - \frac{\partial T}{\partial \beta} = M - \frac{\partial \Pi}{\partial \beta} - \frac{\partial R}{\partial \dot{\beta}};$$

$$\frac{d}{dt}\frac{\partial T}{\partial \dot{u}} - \frac{\partial T}{\partial u} = F - \frac{\partial \Pi}{\partial u} - \frac{\partial R}{\partial \dot{u}};$$

$$\frac{d}{dt}\frac{\partial T}{\partial \dot{x}} - \frac{\partial T}{\partial x} = -F_0 - \frac{\partial \Pi}{\partial x} - \frac{\partial R}{\partial \dot{x}}.$$
(16)

where T and  $\Pi$  are the kinetic and potential energy, respectively, and R is the Rayleigh dissipation function of the integrated crane-winch system for timber extraction; M is the driving torque of the winch drive, reduced to the axis of the drive drum;  $F_0$  is the force resisting the log displacement; F is the component of the rope tension force that causes transverse deformation of the boom.

The kinetic energy of the integrated crane-winch system is expressed as follows

$$T = \frac{1}{2}J\dot{\beta}^2 + \frac{1}{2}m_n\dot{u}^2 + \frac{1}{2}m\dot{x}^2 \tag{17}$$

where J is the moment of inertia of the drive mechanism, reduced to the axis of the drive drum;  $m_n$  is the equivalent mass of the forest crane boom, reduced to the attachment axis of the guiding pulley; m is the mass of the log.

The potential energy of the integrated crane-winch system is expressed by the following relation

$$\Pi = \frac{1}{2}c_n u^2 + \frac{1}{2}c\left(\beta r - \frac{x}{\cos\alpha}\right)^2 + mg\left(\frac{d_k}{2\cos\lambda} + x\sin\lambda\right),$$
(18)

where *r* is the radius of the winch drum.

The Rayleigh dissipation function for the considered system is given by

$$R = \frac{1}{2}b\left(\dot{\beta}r - \frac{\dot{x}}{\cos\alpha}\right)^2 + \frac{1}{2}b_n\dot{u}^2\tag{19}$$

where b and  $b_n$  are the damping coefficients of the traction rope and the loader boom, respectively. The values for these damping coefficients  $(b, b_n)$  were obtained from previous experimental studies on analogous crane and robotic systems, and correlate well with results from com-bined theoretical-experimental methods.

As a result of substituting expressions Eqs. (13) – (15) and Eqs. (17) – (19) into the system of Eqs. (16), the mathematical model of the dynamic motion of the integrated system for timber extraction is obtained:

$$J\ddot{\beta} = \left[ M_p + \left( K \omega_0 - \frac{M_p}{\omega_0} \right) u \dot{\beta} - K(u \dot{\beta})^2 \right] u \eta -$$

$$-cr \left( \beta r - \frac{x}{\cos \alpha} \right) - br \left( \dot{\beta} r - \frac{\dot{x}}{\cos \alpha} \right);$$

$$m_n \ddot{u} = cr \left( \beta r - \frac{x}{\cos \alpha} \right) \cos \theta - c_n u - b_n \dot{u};$$

$$c \left( \beta r - \frac{x}{\cos \alpha} \right)$$

$$m \ddot{x} = \frac{c \left( \beta r - \frac{x}{\cos \alpha} \right)}{\cos \alpha - mg} \left[ \sin \lambda + f_0 \left( \frac{\cos \lambda - \frac{x}{\cos \alpha}}{f_0 \cdot \sin \lambda + \cos \lambda} \sin \alpha \right) \right] +$$

$$+ \frac{b \left( \dot{\beta} r - \frac{\dot{x}}{\cos \alpha} \right)}{\cos \alpha}.$$

$$(20)$$

#### 5. RESULTS AND DISCUSSION

#### 5.1 Results of Simulation

The obtained system represents a set of three nonlinear second-order differential equations that cannot be solved analytically. Therefore, numerical methods, particularly in the form of computer programs, must be employed to obtain the solution. The differential Eqs. (20) are solved under the following initial motion conditions:

$$t = 0; \ \beta = \frac{S_{k0}}{cr}; \ \dot{\beta} = 0; \ u = S_{k0} \cos \theta; \ \dot{u} = 0;$$
  
 $x = 0; \ \dot{x} = 0,$  (21)

where  $S_{k0}$  denotes the tension force in the traction rope at the initial moment of motion.

For the integrated hydraulic forest crane-winch system with parameters m = 1280 kg,  $m_n = 364.5$  kg, J = 1.938 kg·m<sup>2</sup>;  $c = 4.082 \cdot 10^5 \frac{\text{N}}{\text{m}}$ ;  $c_n = 1.349 \cdot 10^6 \frac{\text{N}}{\text{m}}$ ;  $f_0 = 1.349 \cdot 10^6 \frac{\text{N}}{\text{m}}$ 

0.70; 
$$u = 39.77$$
;  $\eta = 0.875$ ;  $b = 510 \frac{N}{m/s}$ ;  $b_n = 260$ 

$$\frac{N}{m/s}$$
;  $\omega_0 = 267.28 \frac{\text{rad}}{\text{s}}$ ;  $\omega_n = 238.64 \frac{\text{rad}}{\text{s}}$ ;  $M_n = 37.34$ 

N·m; 
$$M_p = 83.34$$
 H·m;  $r = 0.1$  m;  $g = 9.81 \frac{\text{m}}{\text{s}^2}$ ;  $\lambda =$ 

0.0872 rad;  $\theta = 0.2617$  rad;  $\beta = 0.109$  rad, Eqs. (20) were solved under the initial conditions Eqs. (21). As a result, the kinematic, dynamic, and energy characteristics for the integrated hydraulic forest crane-winch system used for timber extraction were obtained.

Based on the analysis of the graph of changes in the speed of the drive drum (Figure 5), it was found that the angular velocity of the drive drum instantaneously increases to 6.1 rad/s, after which high-frequency oscillations of the drum's angular velocity emerge. These oscillations decay within 4.0 s, resulting in the drive drum rotating at a constant angular velocity of 6.2 rad/s. The maximum angular velocity occurs at the moment of start-up and reaches 6.8 rad/s. In this case, the peak velocity exceeds its steady-state value by only

10%. The instantaneous increase in the drum's angular velocity is caused by the excessive starting torque of the hydraulic drive motor.

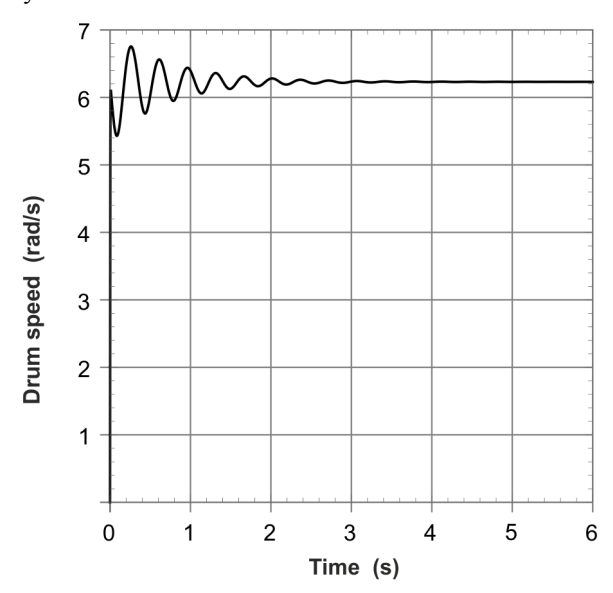


Figure 5. Graph of drive drum speed variation

A similar pattern is observed based on analysis of results in a velocity fluctuation of the equivalent boom mass (Figure 6). Here, high-frequency oscillations are also present, gradually decaying over time. However, these oscillations are multi-frequency, as seen in Figure 5, where multiple vibration modes overlap. The maximum amplitude of the equivalent boom mass velocity oscillations occurs at the initial stage of motion and lasts for 0.30 s. By the twelfth second of system motion, the oscillation amplitude decreases to less than 0.01 m/s.

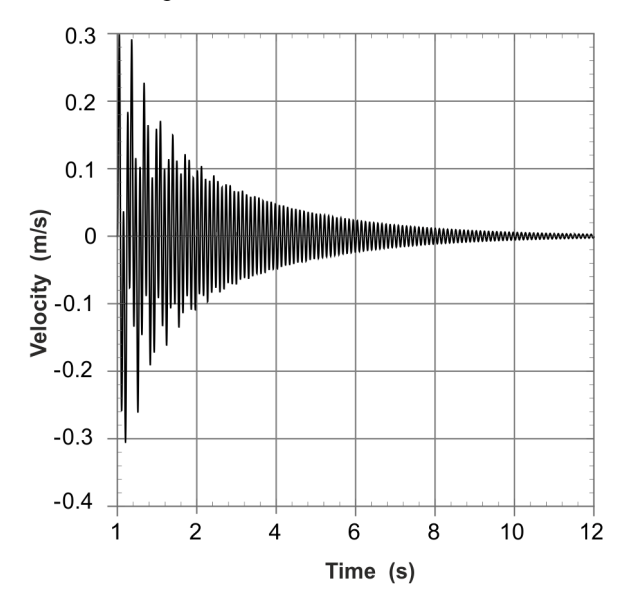


Figure 6. Graph of equivalent boom mass velocity variation

At the initial stage of motion, the log velocity exhibits an oscillatory behaviour (Figure 7), with these oscillations fully decaying by the sixth second. After this period, the log moves at a constant velocity without oscillations. The maximum amplitude of the velocity oscillations occurs at the beginning of motion and reaches 0.60 m/s, while the peak velocity at this moment is 1.20 m/s. The steady-state velocity of the log

is 0.61 m/s. The maximum velocity exceeds the steady-state value by a factor of 1.97. The oscillatory nature of the log velocity variation resulted in an almost twofold increase in its peak velocity compared to the steady-state velocity.

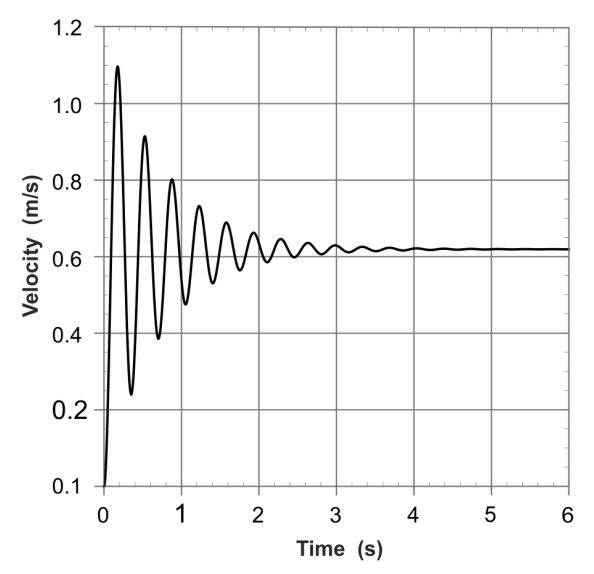


Figure 7. Graph of log velocity variation

Figures 8 and 9 present the phase portraits of the oscillations of the equivalent boom mass and the log, respectively. Each of these phase portraits demonstrates that the oscillations of both the equivalent boom mass and the log are damped. The oscillations of the log are close to sinusoidal damped vibrations, while the oscillations of the equivalent boom mass exhibit a multifrequency nature. During the oscillations of the log, the maximum deformation of the rope reaches 0.6 m at the initial stage, with a maximum deformation velocity of 0.054 m/s. Meanwhile, the maximum deformation of the boom's elastic element reaches 0.020 m, with a peak deformation velocity of 0.32 m/s. These results indicate that, during the oscillations of the integrated cranewinch system components, the wire rope undergoes a greater value of the maximum deformation but has a lower deformation velocity compared to the boom.

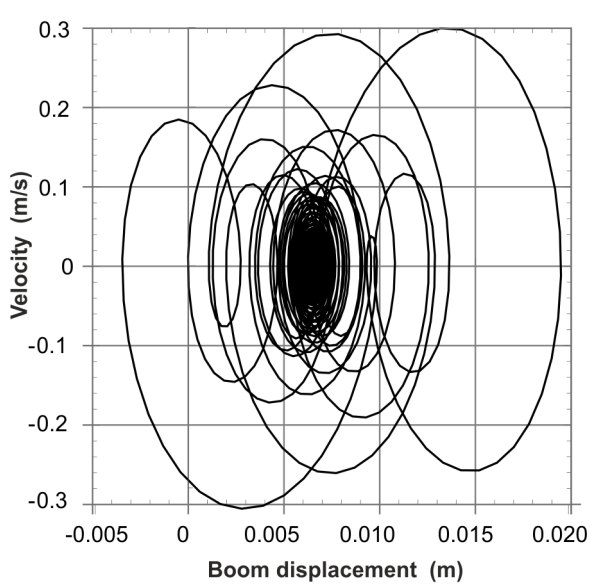


Figure 8. Phase portrait of the equivalent boom mass oscillations

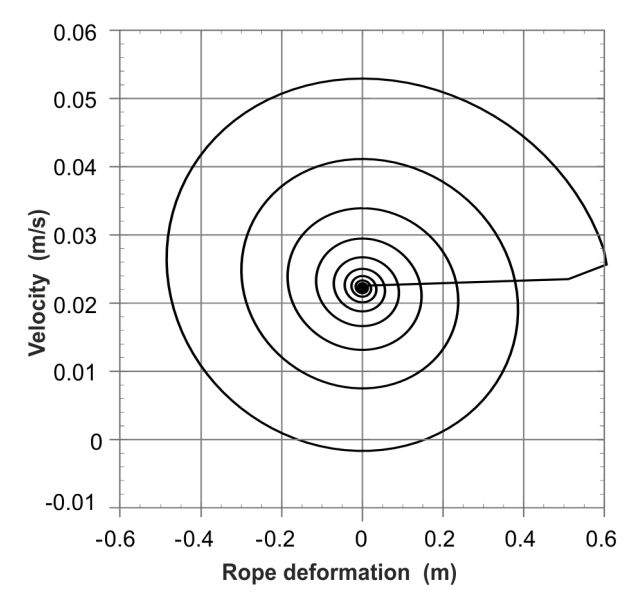


Figure 9. Phase portrait of the log oscillations

At the initial stage of motion, the driving torque on the shaft of the winch drum (Figure 10) instantaneously reaches a peak value of 4.25 kNm and then rapidly drops to 1,15 kNm. Subsequently, it oscillates within the range of 2.20 kNm at the beginning of motion to a steady-state value of 0.95 kNm, which is reached closer to the sixth second of motion. The peak torque exceeds its steady-state value by a factor of 4.47. These results highlight significant dynamic overloading of the winch drive mechanism components during the start-up phase.

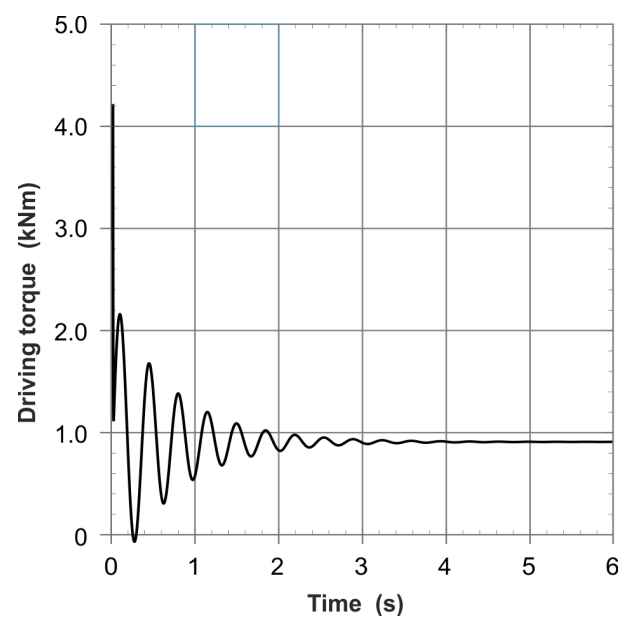


Figure 10. Graph of the drive mechanism torque variation

The tension force in the traction wire rope (Figure 11) varies in an oscillatory mode during the start-up of the drive mechanism, ranging from a peak value of 22.0 kN at the start of motion to a steady-state value of 9.0 kN, which stabilises around the sixth second. At the same time, the peak meaning of the tension force exceeds its steady-state value by a factor of 2.44, indicating that the oscillatory motion of the system leads to rope overloading.

The force in the elastic element of the boom (Figure 12) also varies in a high-frequency damped oscillatory

mode. In this case, the force oscillations exhibit a multifrequency nature, as Figure 12 shows the superposition of multiple vibration modes.

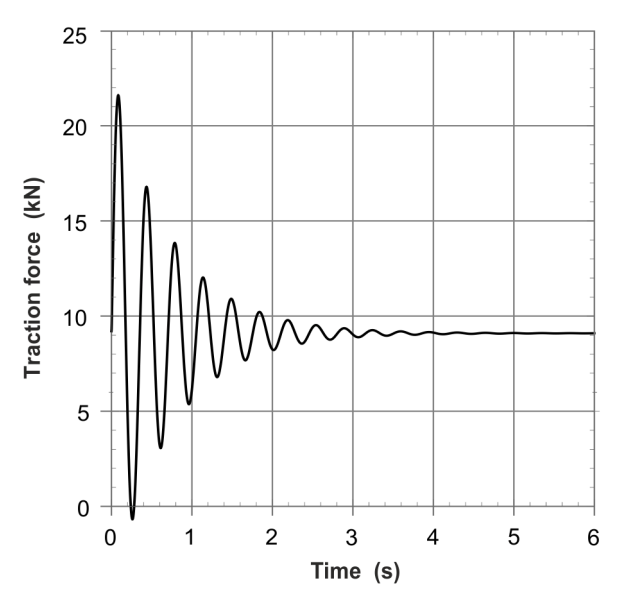


Figure 11. Graph of traction force variation in the rope

The maximum force in the elastic-dissipative element of the boom reaches 26.5 kN at the initial stage of the drive mechanism's motion and nearly attains its steady-state value of 9.1 kN by the twelfth second of motion. Here, the peak value of the force exceeds the steady-state value by a factor of 2.91. The obtained results indicate significant dynamic overloading of the forest crane boom during log movement, with peak load values nearly three times higher than the steady-state value.

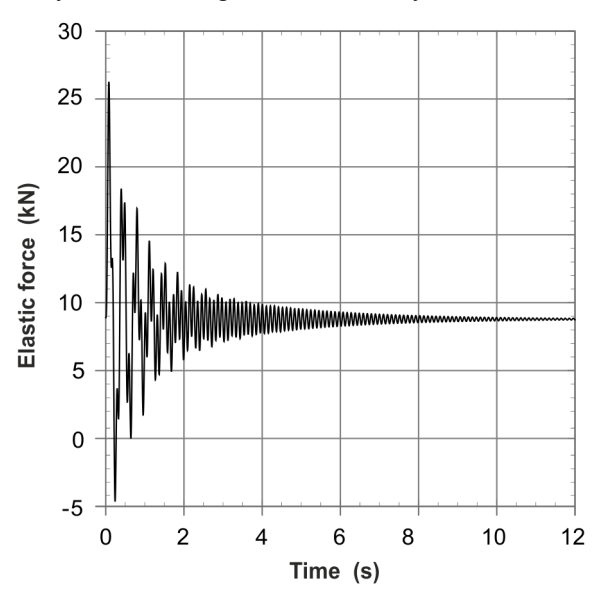


Figure 12. Graph of force variation in the elastic-dissipative element of the equivalent boom mass

# 6. DISCUSSION

The results of dynamic analysis presented in Table 1 reveal several key characteristics of the integrated crane-winch system during the critical timber extraction start-up phase. The substantial transient amplification factors (expressed as multiples of steady-state loads) observed for drive torque 4.47, rope tension 2.44, and

equivalent boom force 2.91 clearly quantify the significant dynamic overloading experienced by the system components compared to their steady-state operational loads. While direct quantitative comparison with literature is complex due to system-specific parameters, these high initial peaks are qualitatively consistent with documented dynamic load fluctuations inherent in hydraulically actuated machinery during acceleration phases [14,16] and winch-assist operations involving abrupt load changes or activations [1,8,24]. The magnitude of the rope tension amplification 2.44, in particular, underscores the necessity of incorporating dynamic load factors in wire rope selection and safety assessments relative to the Safe Working Load [19,33].

Table 1. Key Dynamic Analysis Results During System Start-Up

System Characteristic	Peak Value	Steady- State Value	Over– shoot Factor	Time to Damping / Stabili– sation
Angular velocity of the drive drum	6.8 rad/s	6.2 rad/s	≈1.10 (10% excess)	Within 4.0
Velocity of the equivalent boom mass	±0.3 m/s	≈0 m/s	-	Amplitude < 0.01 m/s by 12 s
Velocity of the log	1.20 m/s	0.61 m/s	1.97	Fully decayed by 6th s
Deformation of the rope	0.6 m	-	-	-
Deformation velocity of the rope	0.054 m/s	-	-	-
Deformation of the boom's elastic element	0.020 m	-	-	-
Peak deformation velocity of the boom's elastic element	0.32 m/s	1	-	•
Driving torque (on the shaft of the winch drum)	4.25 kNm	0.95 kNm	4.47	Reaches steady-state near 6th s
Tension force in the traction wire rope	22.0 kN	9.0 kN	2.44	Stabilises around 6th s
Force in the elastic element of the boom	26.5 kN	9.1 kN	2.91	Attains steady-state by 12th s

Furthermore, the distinct oscillatory behaviours observed – the high-frequency, rapidly damped, multimode vibrations within the drive mechanism and boom structure versus the lower-frequency, more persistent, near-sinusoidal sway of the suspended log – align well with theoretical expectations and findings from previous studies on crane and cable systems [3, 11, 40]. This dichotomy reflects the different sources of excitation and the inherent differences in stiffness and damping between the mechanical structure/drive and the payload system. The relatively swift damping of the high-

frequency structural oscillations highlights the role of inherent structural damping and potential dissipative effects within the hydraulic system [22, 25], whereas the prolonged log sway indicates lower damping, potentially dominated by resistance and/or friction at the log-ground interface (implicitly included in  $F_0$ ).

The analysis strongly implicates the modelled abrupt start-up profile of the hydraulic motor torque Eq. (14) as the primary excitation source for the observed transient phenomena. This rapid torque variation induces the initial overshoot and subsequent high-frequency oscillations in the drive system, which, in turn, excite vibrations in the boom's elastic element and contribute to the initial peak in wire rope tension. This finding reinforces the conclusions drawn in other studies advocating for optimised, smoother start-up protocols or torque profiles to mitigate mechanical stress and reduce energy consumption in loading equipment [15,40,41]. The results provide quantitative evidence supporting the need for such strategies in integrated timber extraction systems.

While the lumped-parameter single-degree-of-freedom model effectively captures the dominant low-frequency boom vibrations and overall transient behaviour, it inherently simplifies the complex distributed flexibility of the actual structure. Higher-order vibration modes or localised stress concentrations would require more detailed modelling approaches, such as FEM, although likely at a significantly higher computational cost [7,25,26]. Similarly, treating the wire rope as extensible when calculating payload dynamics, while commonly used for focusing on swing behaviour, does not fully capture the potential effects of longitudinal rope vibrations, which could interact with the system, especially under high tension or during rapid changes. These modelling choices represent a necessary trade-off between fidelity and tractability for the specific focus on start-up dynamics within this study.

#### 7. CONCLUSION

As a result of the conducted research on the dynamic work of the extraction system for pulling up timber logs, developed based on a forest crane with a hydraulic drive, the following conclusions have been drawn:

- 1. A dynamic model of the extraction system for pulling up logs has been developed. The dynamic model accounts for the characteristic primary motion of the winch drive mechanism and describes the high-frequency oscillations of the traction rope and the forest crane boom, which exhibit elastic-dissipative properties. A mathematical model for the driving torque of the hydraulic motor of the winch drive mechanism has been selected, and the resistance force opposing the log displacement has been determined. Based on the developed dynamic model of the timber extraction system, a mathematical model has been constructed using the Lagrange equations of the second kind. This model represents a system of nonlinear second-order diffe-rential equations. The system of equations was solved numerically using a custom-developed computer program.
- 2. The results of solving the mathematical model enabled a dynamic analysis of the transient process

during the start-up of the timber extraction system for pulling up timber logs. The conducted dynamic analysis revealed significant dynamic loads in the drive components, traction rope, and the structure of the loader boom during the start-up process. The maximum driving torque of the hydraulic drive was found to significantly exceed its steady-state value. The abrupt change in the driving torque of the drive resulted in the emergence of high-frequency oscillations, which affected the kinematic and dynamic characteristics of the extraction system components. The presence of high-frequency oscillations caused considerable dynamic overloading of the forest crane boom and the traction rope of the winch.

3. As a result of the dynamic analysis conducted during the start-up of the extraction system for pulling up timber logs, it was found that the cause of oscillatory processes in the system components is the rapid variation in the driving torque. To reduce or completely eliminate oscillatory processes in the timber extraction system components, it is necessary to implement a smo-oth variation in the driving torque of the drive mecha-nism.

Therefore, the study provides a new integrated dynamic model of a hydraulic forest crane-winch system that simultaneously captures winch drive dynamics, boom flexibility and rope-payload interactions through a coupled Lagrangian formulation with three degrees of freedom. This approach enables the quantitative prediction of transient overload factors for critical components, drive torque, rope tension and boom elastic forces, under realistic start-up conditions. From a practical engineering perspective, the results supply design-oriented guidelines for sizing winch drives and wire ropes, selecting damping elements, and defining smooth start-up torque profiles to reduce mechanical stress and extend service life. The modelling framework can be directly applied to the design, optimisation and control of modern forest-harvesting equipment and other cable-assisted material-handling machines operating in variable terrain.

# **REFERENCES**

- [1] O. Mologni, E. D. T. Nance, C. K. Lyons, L. Marchi, S. Grigolato, R. Cavalli, D. Roeser, "Cable Tensile Forces Associated to Winch Design in Tethered Harvesting Operations: A Case Study from the Pacific North West," Forests, vol. 12, no. 7, id. 827, pp.1–15, 2021, doi: 10.3390/f12070827.
- [2] G. Erber, R. Spinelli, "Timber extraction by cable yarding on flat and wet terrain: a survey of cable yarder manufacturer's experience," Silva Fennica, vol. 54, no. 2, pp. 1–19, 2020, doi: 10.14214/sf.10211.
- [3] J. Schweier, C. Ludowicy. "Comparison of A Cable-Based and a Ground-Based System in Flat and Soil-Sensitive Area: A Case Study from Southern Baden in Germany," Forests, vol. 11, no. 6, id 611, pp. 1–16, 2020, doi: 10.3390/f11060611.
- [4] S. A. Borz, A-C. Mariş, N. Kaakkurivaara. "Performance of Skidding Operations in Low-Access and Low-Intensity Timber Removals: A Simulation of Productivity and Fuel Consumption in Mature

- Forests," Forests, vol. 14. no. 2, id 265, pp.1–16, 2023, doi: 10.3390/f14020265.
- [5] N. Gülci, A. Akay, O. Erdaş, "Optimal planning of timber extraction methods using analytic hierarchy process," European Journal of Forest Research, vol. 139, pp. 647–654, 2020, doi: 10.1007/s10342-020-01275-7.
- [6] O. Mologni, P. Dyson, D. Amishev, A. R. Proto, G. Zimbalatti, R. Cavalli, S. Grigolato, "Tensile Force Monitoring on Large Winch-Assist Forwarders Operating in British Columbia," Croatian Journal of Forest Engineering, vol. 39, no. 2, pp. 193–204, 2018, [Online]. Available: https://hrcak.srce.hr/204187.
- [7] P. La Hera, and D. Ortíz Morales, "Model-Based Development of Control Systems for Forestry Cranes," Journal of Control Science and Engineering, Article ID 256951, pp. 1–15, 2015, doi: 10.1155/2015/256951.
- [8] Cook, J. T., Ray, L. E., Lever, J. H. (May 8, 2019). "Mobility Enhancement of Heavy-Duty Tracked Vehicles Under Load Using Real-Time Terrain Characterization, Traction Control, and a Towing Winch", ASME. Journal of Dynamic Systems, Measurement, and Control, vol. 141, no. 7, id 071016, pp. 1–13, 2019, doi: 10.1115/1.4043111.
- [9] N. Gülci, A. E. Akay, O. Erdaş, H. H. Acar, "Productivity Analysis of Chute System integrated with Portable Winch and Synthetic Rope for Uphill Logging Operation," European Journal of Forest Engineering, vol. 3, no. 2, pp. 72–77, 2017.
- [10] D. Rupar, J. Hladnik, B. Jerman, "Loader Crane Inertial forces," FME Transactions, vol. 44, no. 3, pp. 291-297, 2016, doi: 10.5937/fmet1603291R.
- [11] V. S. Loveikin, Yu. O. Romasevych, A. V. Loveikin, A. P. Liashko, and K. I. Pochka. "Dynamic analysis of the simultaneous starting of the boom and load lifting mechanisms hoisting for the jib and the cargo of the jib crane with a hydraulic drive," Strength of Materials and Theory of Structures. no. 113, pp. 149-160, 2024, doi: 10.32347/2410-2547.2024.113.149-160.
- [12] B. Mahura, B. Bakay, O. Bilous, I. Karatnyk, V. Kiy, "Determining the optimal angle of traction force application of a "walking sledge" skidding device," Bulletin of Kharkov National Automobile and Highway University, vol. 101, no. 2, pp. 121–128, 2023, doi: 10.30977/BUL.2219-5548.2023. 101.2.121–128.
- [13] E. Jelavić, D. Jud, P. Egli, M. Hutter, "Robotic Precision Harvesting: Mapping, Localization, Planning and Control for a Legged Tree," Field Robotics, vol. 2, pp. 1386–1431, 2022, doi: 10.55417/fr.202 2046.
- [14] E. Papadopoulos, S. Sarkar, "The dynamics of an articulated forestry machine and its applications," in Proceedings of International Conference on Robotics and Automation, Albuquerque, NM, USA, pp. 323–328 vol. 1, 1997. doi: 10.1109/ROBOT. 1997.620058.

- [15] V. Loveikin, Y. Romasevych, Y. Loveikin, V. Krushelnytskyi, I. Kadykalo, "Optimization of the joint startup of the boom and load hoisting mechanisms of a jib crane," Machinery & Energetics, vol. 15, no. 4, pp. 9–21, 2024, doi: 10.31548/machinery/4.2024.09.
- [16] P. La Hera, B. Ur Rehman, D. Ortíz Morales, "Electro-hydraulically actuated forestry manipulator: Modeling and Identification," in 2012 IEEE/RSJ International Conference on Intelligent Robots and Systems, Vilamoura-Algarve, Portugal, pp. 3399–3404, 2012, doi: 10.1109/IROS.2012.6385 656.M.
- [17] M. Kodrič, J. Flašker, S. Pehan, "Efficiency Improvement of Agricultural Winch Machines," Strojniški vestnik Journal of Mechanical Engineering, vol. 63, no. 3, pp. 171–180, 2017, doi: 10.5545/svjme.2016.3968.
- [18] S. K. Dwivedy, P. Eberhard, "Dynamic analysis of flexible manipulators, a literature review," Mechanism and Machine Theory, vol. 41, no. 7, pp. 749–777, 2006, doi: 10.1016/j.mechmachtheory. 2006.01.014.
- [19] Ireland D. and Great Britain. Forestry Commission. "Winching Operations in Forestry: Tree Takedown and Vehicle Debogging," Edinburgh; 2004.
- [20] M. H. Adamowskij and B. Y. Bakay, "Analysis and prospect of the use of skidding tractors in the forest complex of Ukraine," Scientific bulletin of UNFU, vol. 14, no. 3, pp. 175–182, 2004. Available: https://nv.nltu.edu.ua/Archive/2004/14\_3/34.pdf.
- [21] P. Beno, J. Krilek, J. Kovač, D. Kozak, C. Fragassa, "The Analysis of the New Conception Transportation Cableway System Based on the Tractor Equipment," FME Transactions, vol. 46, no. 1; pp. 17-22, 2018, doi: 10.5937/fmet1801017B.
- [22] P. X. La Hera, D. Ortíz Morales, "What Do We Observe When We Equip a Forestry Crane with Motion Sensors?," Croatian journal of forest engineering, vol. 40, no. 2, pp. 259–280, 2019, doi: 10.5552/crojfe.2019.501.
- [23] M. Yoshida, H. Sakai, "Winch Harvesting on Flat and Steep Terrain Areas and Improvement of its Methodology," Croatian Journal of Forest Engineering, vol. 36, no. 1, pp. 55–61, 2015.
- [24] T. Farsakoglou, H. C. Pedersen, T. O. Andersen, "Review of offshore winch drive topologies and control methods," in The 13th International Fluid Power Conference: 13 IFK, 2022. doi:10.18154/ RWTH2023-04600.
- [25] E. Papadopoulos, B. Mu, R. Frenette, "Modeling and identification of an electrohydraulic articulated forestry machine," in Proceedings of International Conference on Robotics and Automation, Albuquerque, NM, USA, vol. 1, pp. 60–65, 1997, doi: 10.1109/ROBOT.1997.620016.
- [26] D. Subedi, I. Tyapin, G. Hovland, "Review on Modeling and Control of Flexible Link Manipulators", Modeling, Identification and Control,

- vol. 41, no. 3, pp. 141-163, 2020, doi:10.4173/mic.2020.3.2.
- [27] N. Mishra, S.P. Singh, "Dynamic modelling and control of flexible link manipulators: methods and scope- Part-1," Indian Journal of Science and Technology, vol. 14, no. 43, pp. 3210–3226, 2021, doi: 10.17485/IJST/v14i43.1418-I.
- [28] M. Sayahkarajy, Z. Mohamed, A. A. M. Faudzi. "Review of modelling and control of flexible-link manipulators," Proceedings of the Institution of Mechanical Engineers, Part I: Journal of Systems and Control Engineering, vol. 230, no. 8, pp. 861–873, 2016, doi: 10.1177/0959651816642099.
- [29]B. Ya. Bakay, "Preliminary representation of the equation of dynamics of the manipulator by method Euler-Lagrange," Scientific bulletin of UNFU, vol. 21, no. 18, pp. 322–327, 2011, [Online]. Available: https://nv.nltu.edu.ua/Archive/2011/21\_18/322\_Bak.pdf.
- [30] L. V. Duong, L. A. Tuan, "Modeling and observer-based robust controllers for telescopic truck cranes", Mechanism and Machine Theory, vol. 173, pp. 104869, 2022, doi: 10.1016/j.mechmachtheory. 2022.104869.
- [31] A. Urbaś, "Mathematical description of a flexible connection of links and its applications in modeling the joints of spatial linkage mechanisms", Latin American Journal of Solids and Structures, vol. 13, no. 15, pp. 2896–2921, 2016, doi: 10.1590/1679-78252673.
- [32]B. Koo, S.-M. Chang, S. Kang, "Natural mode analysis of a telescopic boom system with multiple sections using the Rayleigh-Ritz method," Journal of Mechanical Science and Technology, vol. 32, no. 4, pp. 1677–1684, 2018, doi: 10.1007/s12206-018-0324-4.
- [33] A. Urbaś, K. Augustynek, J. Stadnicki, "Dynamics analysis of a crane with consideration of a load geometry and a rope sling system," Journal of Sound and Vibration, vol. 572, pp. 118–133, 2024, doi: 10.1016/j.jsv.2023.118133.
- [34] Y. Franco, A. Degani, "Modeling of rigid-link and compliant joint manipulator using the discrete body dynamics method," Multibody System Dynamics, vol. 61, pp. 1–18, 2024, doi: 10.1007/s11044-023-09897-6.
- [35] P. X. La Hera, D. Ortíz Morales, "Non-linear dynamics modelling description for simulating the behaviour of forestry cranes," International Journal of Modelling, Identification and Control, vol. 21, no. 2, 2014, pp. 125–138, doi: 10.1504/IJMIC.2014.060006.
- [36] I. M. Abu-Alshaikh, A. N. Al-Rabadi, H. S. Alkhaldi, "Dynamic Response of Beam with Multi-Attached Oscillators and Moving Mass: Fractional Calculus Approach," Jordan Journal of Mechanical and Industrial Engineering, vol. 8, no. 5, pp. 275–288, 2014.
- [37] A. Urbaś, "Computational implementation of the rigid finite element method in the statics and dy-

- namics analysis of forest cranes," Applied Mathematical Modelling, vol. 46, pp. 750-762, 2017, doi: 10.1016/j.apm.2016.08.006.
- [38] X. Chen, L. Bing, L. Guigao, "Numerical Simulation Research on the Anchor Last Deployment of Marine Submersible Buoy System Based on VOF Method," Journal of Marine Science and Engineering, vol. 10, no. 11: pp. 1681, 2022, doi:10. 3390/jmse10111681.
- [39] T. H. Evang, S. Skjong, E. Pedersen, "Crane Rig: An Experimental Setup for Developing and Verifying New Control Methods for Marine Crane Operations," in Proceedings of the ASME 2017 36th International Conference on Ocean, Offshore and Arctic Engineering, vol. 7A: Ocean Engineering. Trondheim, Norway, 2017. doi: 10.1115/ OMAE2017-62010.
- [40] V. S. Loveikin, Yu. O. Romasevych, A. V. Loveikin, and A. S. Khoroshun. "Optimizing the Start of the Trolley Mechanism during Steady Slewing of Tower Crane". International Applied Mechanics, vol. 58, no. 5, pp. 594–604, 2022, doi: 10.1007/s10778-023-01183-4.
- [41] S. Chwastek, "Optimization of Crane Mechanisms to Reduce Vibration," Automation in Construction, vol. 119, pp. 1–9, 2020, doi: 10.1016/j.autcon. 2020.103335.

#### **NOMENCLATURE**

#### Latin symbols

- a Distance to the location of the pulley
- $b_1$  Distance to the location of the traction winch
- L Boom length of the forest crane
- EI Boom stiffness
- E Modulus of elasticity of steel
- Boom cross-sectional moment of inertia
  - (about bending axis)
- $m_n$  Equivalent discrete boom mass
- z Generalised boom coordinate
- $c_n$  Generalised boom stiffness
- $m^*$  Boom generalized mass at midspan
- $c^*$  Boom generalized stiffness at midspan
- M Winch drive driving torque
- J Winch drive moment of inertia
- $c_n$  Stiffness coefficient
- $b_n$  Damping coefficient
- c Rope stiffness coefficient
- b Rope damping coefficient
- $S_k$  Rope tension force
- m Log mass
- $F_0$  Resistance force to log motion
- $E_k$  Rope elastic modulus
- d Rope diameter
- $L_k$  Variable rope length
- $S_r$  Rope cross-sectional area
- $f_0$  Log motion resistance coefficient

$g$ $M_p$	Gravitational acceleration Hydraulic motor starting torque
$M_n$	Hydraulic motor nominal torque
$i_w$	Winch drive transmission ratio
u	Boom deformation linear coordinate at guiding pulley attachment point
$\boldsymbol{x}$	Log displacement linear coordinate
T	Kinetic energy
R	Rayleigh dissipation function
F	Rope tension force component
r	Winch drum radius
b	Traction rope damping coefficient
$b_n$	Loader boom damping coefficient

# Greek symbols

 $S_{k0}$ 

$\psi$	Mode shape
λ	Terrain inclination angle

 $\alpha$  Rope inclination angle relative to log motion

Initial traction rope tension force

direction

 $\omega_n$  Hydraulic motor shaft nominal angular velocity

 $\omega_0$  Hydraulic motor shaft synchronous angular

η Winch drive efficiency

 $\beta$  Drive drum angular coordinate

Π Potential energy

#### Acronyms and Abbreviations

AMM	assumed modes method
FEM	finite element method
LPM	lumped parameter method
TMM	transfer matrix method
ODEs	ordinary differential equations

# МОДЕЛИРАЊЕ И ДИНАМИЧКА АНАЛИЗА ИНТЕГРИСАНОГ ХИДРАУЛИЧКОГ ШУМСКОГ КРАНА-ЧЕКРКА ЗА ИЗВЛАЧЕЊЕ ДРВЕТА

## В. Ловејкин, Ј. Ромасевич, Б. Бакај, И. Рудко, И. Радјак

Овај рад детаљно описује динамичко моделирање и анализу интегрисаног хидрауличког шумског краначекрка који се користи за извлачење дрвета, с фокусом на прелазно понашање током активације чекрка из мировања. Развијен је свеобухватан математички модел коришћењем Лагранжеве формулације за спрегнуту динамику система, који је нумерички решен помоћу прилагођених алгоритама због своје нелинеарности. Динамичка анализа је открила значајно прелазно преоптерећење компоненти: максимални обртни момент погона, затегнутост ужета и еластична сила гране крана премашили су устаљене вредности за факторе од 4,47, 2,44 и 2,91, респективно.

Идентификоване су брзо пригушене високофреквенцијске осцилације у структури крана и погону (које се стабилизују за око 4 секунде) суперпониране на нискофреквенцијско љуљање терета, што се приписује наглом довођењу обртног момента погона. Ово истраживање наглашава неопходност динамичке анализе за предвиђање значајног пораста напрезања и ризика од замора компоненти. Резултати јасно указују на то да су стратегије равномернијег покретања кључне за повећање поузданости и ефикасности система током критичних фаза операције.